Opening the door to liquid-free polymer electrolytes for calcium batteries

C.S. Martinez-Cisneros, A. Fernandez, C. Antonelli, B. Levenfeld, A. Varez, K. Vezzù, V. Di Noto, J.-Y. Sanchez

Opening the door to liquid-free polymer electrolytes for calcium batteries

C.S. Martinez-Cisneros[1], A. Fernandez[1], C. Antonelli[2], B. Levenfeld[1], A. Varez[1], K. Vezzù[3], V. Di Noto[1,3], J-Y. Sanchez[1,4*]

[1] Materials Science and Engineering Department, University Carlos III of Madrid, Spain.

[2] Institut Européen des membranes (IEM), UMR-5635, Université de Montpellier, ENSCM, CNRS, Place Eugène Bataillon, 34095 Montpellier cedex 5, France.

[3] Section of Chemistry for Technologies (ChemTec), Department of Industrial Engineering, University of Padova, Via Marzolo 9, 35131 Padova (PD), Italy.

[4] UJF UdS, Grenoble INP, LEPMI, UMRCNRS5279, 1130 Rue Piscine, BP75, F-38402 S[t] Martin d'Hères, France.

Abstract

This work studies calcium-conducting, solvent-free polymer electrolytes in the framework of today's post-lithium battery strategies. The samples consist of three calcium salts: (i) $Ca(CF_3SO_3)_2$; (ii) $Ca(TFSI)_2$; and (iii) CaI_2 hosted by commercial poly(oxyethylene) (POE). The data collected from X-ray diffraction (XRD), scanning electron microscopy (SEM), differential scanning calorimetry (DSC) and thermogravimetric analysis (TGA) indicate that the polymer electrolytes consist of stable macromolecular solutions of these calcium salts. The polymer electrolytes yield conductivities exceeding 0.1 $mS{\cdot}cm^{-1}$; POE-$Ca(CF_3SO_3)_2$ reaching, at the moderate concentration O/Ca =30, a conductivity of 0.47 $mS{\cdot}cm^{-1}$. This preliminary and

fundamental study, which demonstrates the stability of Ca-conducting polymer electrolytes, paves the way to the development of improved polymer electrolytes based on oxyethylene repeat units and new calcium salts.

Keywords: Calcium electrolytes; calcium batteries, polymer electrolytes; energy storage; poly(oxyethylene), (POE, PEO).

1. Introduction

The market for batteries, which approached 50 billion $ in 2012 [1], is expected to grow by more than 60% by 2020; such a growth is expected to reach 100% in the case of lithium batteries (LiBs). Long-time confined to portable electronics, the growth of the market for LiBs is driven by those developments achieved in Battery Electric Vehicles (BEVs) and Plug-in-Hybrid Electric Vehicles (PHEVs). The latter are expected to play a crucial role to curtail both greenhouse gas emissions and urban pollution. Indeed, as concerns the automotive market, the Federal Council of Germany voted to ban internal combustion engines (ICEs) by 2030 [2], while in France the ban on ICEs has been placed by 2040 [3]. These decisions are yielding a huge impact on the development strategies of car manufacturers, greatly promoting the diffusion of BEVs and PHEVs. Besides BEV and PHEV, non-mobile grid-levelling applications typically require large-scale energy storage systems to buffer the intermittency of the demand and, in the case of renewable energies such as solar and wind, of the supply of electricity. However, the high cost of LiBs bottlenecks their application as large-scale energy storage systems for the power grid [4]. Hence, the end users require cheaper, safer and more efficient batteries for both electric vehicles and stationary energy storage applications. Such criteria often contradict one another. More efficient: if the electrode materials were changed from

$Li_4Ti_5O_{12}$/$LiFePO_4$ to C/$LiCoO_2$, the battery energy density would increase from 70 to 200 $Wh \cdot kg^{-1}$; however, at the same time, the cyclability of the device would be reduced [5]. Safer: regarding safety, the combustion of a 18650 Li-ion cells releases twice the energy of a TNT grenade by summing the cell energy ca. 0.93 $J \cdot g^{-1}$ and the combustion energy of organic components i.e. solvents, separator and binders [6]. Cheaper: even if the cost of battery packs is constantly decreasing [7], the target of 150 $\$ \cdot kWh^{-1}$ has not been reached yet owing to the material costs and to the processing cost of LiBs [8,[9]. Another handicap suffered by LiBs in the medium term is the shortage of lithium ores, triggered by the huge demand for this energy storage technology. Thus, it is mandatory to devise new batteries where Li is replaced by cheaper elements that are more abundant in Earth's crust, *e.g.*, Na, K, Mg and Ca, whose properties are compared in Table 1.

The ideal solution to devise high-energy density batteries remains based on the implementation of metals at the negative electrode. This approach yields important advantages, as it raises the capacity, the voltage and the energy density of the battery; concurrently, the processing of the battery is simplified and the ohmic losses are reduced. It should be highlighted that calcium and lithium exhibit the same volumetric capacity. Furthermore, calcium is characterized by a very low reduction potential, -2.87 V *vs.* SHE, close to lithium one (-3.05 V *vs.* SHE). In addition, calcium exhibits the highest electrical conductivity among the metals listed in Table 1. On the other hand, one relevant parameter for the battery safety is the melting temperature of the alkaline/alkaline-earth metal anode. Calcium melts at 842°C; this is the highest melting temperature among all the metals listed in Table 1. Hence, it is inferred that a battery based on a calcium metal negative, Ca^0, would provide high capacity and high safety as compared to a graphite electrode, which barely exhibits a reversible capacity of 85 mAhg over 200 cycles and co-intercalates solvent molecules as DMAC [10]. Based on all these pieces of

information, a Ca^0-based calcium battery, CaB, would be a perfect post-lithium alternative. A non-rechargeable CaB, was early proposed by Peled *et al.* [11[12[13], who claimed similar performances than LiB ones and improved safety, but did not succeed in cycling Ca^0. More recently, a 600 mAh/g practical capacity was reported for a Ca^0/S primary CaB [14]. Regarding the cycling issue of Ca^0, Aurbach *et al*. [15] reported the first general study concerning Ca^0 behavior in aprotic organic liquid electrolytes based on $Ca(ClO_4)_2$ where, contrary to Li^0, Ca^{2+} deposition onto Ca^0 did not occur. Post-mortem analyses of the Ca^0 surface revealed the presence of passivation films of $Ca(CO_3)_2$ and $Ca(OH)_2$, which prevent further diffusion of Ca^{2+} and its deposition on Ca^0. For a long time, the deposition of Ca^{2+} onto Ca^0, only occurred at very high temperatures [16[17]. The contribution of Ponrouch *et al.* [18] shows promise results, as it demonstrates the deposition at temperatures in the range of 75-100 °C of Ca^{2+} onto Ca^0 from a liquid electrolyte based on cyclic carbonates. However, this deposition process, observed from cyclic voltammetry measurements, was characterized by a high overpotential and a low capacity. In view of the observed passivation of Ca^0 by $Ca(CO_3)_2$ [15], the selected cyclic carbonates are probably not the most suitable solvents for this application. P.G. Bruce *et al.* [19] recently reported improved calcium deposition/stripping, discarding cyclic and acyclic carbonates but using, as electrolyte, a THF solution of $Ca(BH_4)_2$. In this case, deposition/stripping was observed at room temperature, over 50 cycles with a much lower polarization and a better plating/stripping than those reported by Ponrouch [18]. The formation of CaH_2, with derives from the dehydrogenation of THF into 2, 3-dihydrofuran, was observed on Ca^0. As stated by the authors and pointed out by Ponrouch [20], the electrolyte used in this work exhibits too low anodic stability to be used with a high-potential cathode and the THF solvent undergoes a significant degradation. Therefore, neither carbonates nor THF could allow cycling efficiently calcium batteries. Besides, the

review of Muldoon *et al.* [21] ascribed the lack of interest for CaB to the lack of suitable electrolytes. Can calcium polymer electrolytes, CAPE, become an alternative to liquid ones? First results evidenced fairly high conductivities of Ca salts hosted by solvent-free commercial poly(oxyethylene) POE or *PEO* homopolymer and POE-based amorphous networks [22]. It has been recently reported that highly concentrated polymeric solution of calcium nitrate in poly(oxyethylene) and poly(oxytetramethylene) networks, both obtained by UV insolation [23[24] can provide at high temperature (110ºC) conductivities in excess of 0.1 mS/cm. Regarding CAPE, high conductivity is a necessary but not sufficient condition: it is indeed essential to form stable macromolecular solutions of Ca salts in a wide range of salt concentrations. As a matter of fact, polypropylene oxide, PPO, long time used as an amorphous alternative to POE regarding Infra-Red and Raman studies, was found, a decade later, to undergo microphase separation with several POP/Li salts electrolytes [25]. In this work, we aim at investigating solvent-free polymer electrolytes to pave the way towards the development of sustainable and cheaper batteries with improved safety. As a first approach, we study the features of polymer electrolytes based on a "reference" host polymer, *i.e.*, poly(oxyethylene), POE or PEO, hosting different Ca salts.

2. Experimental

2.1. Materials

Analytical-grade reagents were supplied by Sigma-Aldrich. Poly(oxyethylene) (POE) (M_w $3{\cdot}10^5$ $g{\cdot}mol^{-1}$) was used as the host polymer. In a first approach, calcium trifluoromethane sulfonate, $Ca(CF_3SO_3)_2$, was used to prepare polymer electrolytes at different O/Ca ratios (8, 16, 20, 30, 40). For comparison purposes, calcium polymer electrolytes based on calcium iodide, CaI_2, and calcium

bis(trifluoromethanesulfonyl)imide, $Ca(TFSI)_2$ were also prepared at two O/Ca ratios (30 and 40).

2.2. Preparation of POE-based electrolytes

The green approach previously described [26] is applied to obtain electrolyte films. Briefly, each electrolyte film is obtained by dissolving in deionized water specific amounts of POE and the corresponding calcium salt according to the O/Ca ratios. For instance, in case of the POE-$Ca(CF_3SO_3)_2$ electrolyte (O/Ca=40), 0.19 g of $Ca(CF_3SO_3)_2$ were dissolved in 1g of POE and 10 ml of deionized water. Solutions are stirred for five hours, frozen at -20°C and then lyophilized over the course of 48 hours by means of a FreeZone instrument (LABCONCO, USA). The resulting powders are then deposited on a stainless steel plate and brought to 100°C for 20 minutes; this process: (1) eliminates the residual moisture; and (ii) melts the powders. The melted polymer undergoes hot-pressing at 50 kN and 100°C, resulting in films that exhibit a thickness of 100-150 μm. Films obtained are further dried under vacuum at 50°C for 12 h and stored in a glove box (M. Braun, GmbH, Germany) filled with argon, in which moisture was lower than 1 ppm to prevent any water absorption.

2.3. X-Ray diffraction

X-Ray diffraction (XRD) measurements were carried out using a Philips X'PERT MPD diffractometer (Cu K_α radiation) operating at 40 kV and 40 mA. The XRD patterns were recorded over a 2θ range of 5-80° using a step scan of 0.02° and a counting time of 1 sec per step.

2.4. Scanning Electron Microscopy (SEM)

The distribution of calcium in the electrolytes was studied by using the FEI Teneo Scanning Electron Microscope. For this purpose, X-ray mapping involving the creation of multiple elemental maps was performed at 6 kV and 0.8 nA using the EDAX TEAM™ EDS Analysis System for samples based on $Ca(CF_3SO_3)_2$, CaI_2 and $Ca(TFSI)_2$, all at O/Ca=30.

2.5. Thermal and thermomechanical analyses

The thermogravimetric analysis (TGA) of samples (~8.5 mg) was performed using a Pyris 1 TGA (Perkin Elmer, USA) thermogravimetric analyzer. Samples were heated in a platinum crucible from 30°C to 650°C (at 10°C·min^{-1}) under a nitrogen atmosphere. The onset temperature (T_{onset}) was established as the intersection point between the tangent drawn at the point of highest slope with the extrapolated baseline. Differential scanning calorimetry (DSC) was conducted using a DSC822e (Mettler Toledo, Switzerland) under a 50 mL·min^{-1} constant flow of nitrogen. The melting temperature (T_m) and the enthalpy of fusion (ΔH_m) were estimated between -90°C and 150°C (scan rate: 10°C·min^{-1}). DSC measurements were collected during the second heating scan; the first heating scan removes the thermal history of the samples. The relative percentage of crystallinity (X_c) was directly related to the area under the 1st melting peak by using equation 1 [27]:

$$X_c = \Delta H_m / \Delta H_m^0 \times 100\% \quad \text{(eq. 1)}$$

where ΔH_m is the melting enthalpy estimated experimentally and ΔH^0_m is the melting enthalpy for 100% crystalline POE (213.7 J·g^{-1} [28]). Dynamic Mechanical Thermal Analyses (DMTA) were carried out using a DMA Q800 machine (TA Instruments, USA) working in tensile mode at 1 Hz and at an oscillation amplitude of 15 µm. DMTA samples

were rectangular (2.5 mm x 7.5 mm), with a thickness ranging between 100 and 150 µm. DMTA measurements were performed by heating samples from -100°C to +120°C at a heating rate of 5°C·min^{-1} in air atmosphere.

2.6. Ionic conductivity measurements

Conductivity measurements are collected by Impedance Spectroscopy (IS) using an Impedance/Gain-Phase Analyzer SI1260 (Solartron, UK) and applying a 100 mV amplitude signal in the 1 Hz - 10 MHz frequency range. The measurements were carried out upon heating, at temperatures between 20 and 90°C with a step of 10°C. The samples are sandwiched between stainless steel blocking electrodes (Ø = 11 mm) embedded in a Swagelok-Nylon cell. A dwell time of 30 minutes between measurements was found to be enough for the system to reach a stable temperature.

3. Results and Discussion

Since high molecular weight POEs undergo dramatic chain breaking even as its solutions are mildly sheared [29], we chose the commercial grade having a molecular weight of 300,000 g·mol^{-1}. Among the calcium salts previously used in liquid electrolytes can be quoted $Ca(ClO_4)_2$ [15], $Ca(CF_3SO_3)_2$, $Ca(BF_4)_2$ [18][19]. We discarded $Ca(ClO_4)_2$ for safety reasons and $Ca(BH_4)_2$ because both its limited anodic stability and its expected too low conductivities in non-polar CAPE. As for $Ca(BF_4)_2$ we feared the possible disproportionation of the tetrafluoroborate anion into BF_3 and F^- leading to a highly resistive SEI made of CaF_2. For the same reasons we didn't pay attention to PF_6^- and FSI $[(F\text{-}SO_2)_2]^-$ anions still more likely than BF_4^- to generate CaF_2. Even though C-F bonds can be broken in contact with highly reductive metals as alkaline ones via metal-halogen exchange, we assumed that this reaction would be more limited in aprotic solvent-free

polyether and selected calcium triflate and calcium trifluoromethane sulfonyl imide, both anions exhibiting a high anodic stability. Due to its intrinsic stability in reduction, the third salt, CaI_2, has been selected despite its limited anodic stability (E_0 = 0.54 V *vs.* SHE).

3.1. Microstructural analysis

A thorough characterization by XRD and DSC of POE-$Ca(CF_3SO_3)_2$ salt complexes was previously reported by Mehta *et al.* [31]. XRD was used to characterize crystallinity variations in the POE-$Ca(CF_3SO_3)_2$ polymer electrolytes as related to the concentration of salt. XRD patterns of: (i) pristine, *"salt-free"* POE; (ii) samples with different O/Ca ratios; and (iii) $Ca(CF_3SO_3)_2$ salt are reported in Figure S1 of Supplementary Information.

The homogeneous distribution of calcium in the polymer electrolytes was evaluated by X-ray mapping at room temperature. Three samples with the same salt concentration (O/Ca=30) were investigated, each including a different calcium salt. According to Figure 1, the X-ray mapping does not reveal any heterogeneity in the distribution of calcium, nor the presence of pores. This confirms that the proposed lyophilization/hot-pressing preparation procedure is able to yield highly homogeneous samples.

3.2. Differential scanning calorimetry (DSC)

DSC measurements were performed to elucidate the microstructural variations of the polymer electrolytes as related to the salt concentration and type. In general, the endothermic peaks shown in Figure 2, corresponding to melting temperature T_m, shift to lower temperatures as the concentration of salt raises. The shift of T_m to lower temperatures as the concentration of salt increases is associated to the more amorphous microstructure induced by the polymer/salt interactions. Table 2 summarizes T_m, melting enthalpy (ΔH_m) and crystallinity (X_c) for all calcium polymer electrolytes at different

O/Ca ratios. ΔH_m, decreases as the salt concentration raises. In agreement with XRD, this evidence is consistent with a reduction in the degree of crystallinity.

It can be noticed that T_m and X_c of POE-$Ca(CF_3SO_3)_2$ (O/Ca=20) are lower than those reported for the analogue Na-based polymer electrolytes (*i.e.*, POE-$NaCF_3SO_3$ with O/Na=20) [26]. Such variation could be ascribed to the features of the salts. On one hand, the size of Ca^{2+} and Na^+ cations (coordination number: 6) are comparable (1.14 *vs* 1.13 Å from fluorides; 1 *vs* 0.99 Å from oxides). On the other hand, Ca^{2+} is divalent. Thus, with respect to Na^+, Ca^{2+}: (i) is more likely to undergo interchain cross-solvation; and (ii) is associated to two monovalent $CF_3SO_3^-$ anions instead of only one. Indeed, $CF_3SO_3^-$ are expected to provide an important contribution to modify the microstructure of the polymer electrolyte, facilitating the segmental mobility of the POE macromolecules.

Regarding the effect of the anions of calcium salts, the lowest crystallinity was obtained for POE-$Ca(TFSI)_2$ polymer electrolytes. It is also highlighted that the difference in crystallinity between POE-$Ca(TFSI)_2$ and POE-$Ca(CF_3SO_3)_2$ is markedly lower than that observed between POE-LiTFSI and POE-$LiCF_3SO_3$ [32]. Moreover, T_m values are slightly higher for POE-$Ca(TFSI)_2$ electrolytes. Hence, it is inferred that the main effects influencing the microstructure of POE arise from: (i) the interactions between Ca^{2+} and the POE chains; and (ii) the hindering resulting from Ca^{2+} bivalence (2 anions by cation).

Since the proposed POE-based calcium polymer electrolytes are semi-crystalline, DSC is unable to estimate accurately the glass transition temperature, T_g. Indeed, in these materials the crystalline phase constrains the amorphous phase, providing an *"artificial"* T_g that is not accurate and is not reported in Table 2. Such a limitation could be addressed by supercooling the semi-crystalline polymer electrolyte, quenching the melted electrolyte at a very high speed would impede crystallization processes. However, this is usually not possible with most commercial DSC equipment. The DSC analyses carried

out on the proposed POE-based polymer electrolytes from room temperature to 300°C reveal the presence of an endothermic peak with an onset at 270°C and a maximum at 287°C. In accordance with the results obtained by Metha *et al.* [31], this peak is ascribed to the precipitation of calcium salts out of the liquid polymer electrolyte owing to the negative entropy of dissolution of calcium triflate in POE. This precipitation does not affect the applicability of the proposed calcium polymer electrolytes as it occurs at temperatures that are much higher than the typical operating temperatures of these systems ($T < 100°C$).

3.3. Thermogravimetric analysis (TGA)

Table 3 lists the onset temperatures of: (i) initial weight loss; (ii) residue at 450°C; and (iii) percent (%) of non-volatile residues as compared to the wt% of salts in the various POE-based polymer electrolytes.

The POE host was completely removed as temperature raised above *ca.* 400°C. Hence, the residues detected at higher temperatures can be correlated to the other components included in the POE-based polymer electrolytes, namely the CaX_2 salts. Thus, comparing the residues at 450ºC (roughly the onset of a thermal degradation plateau) with the nominal content of CaX_2 in the polymer electrolytes, it can be deduced that both CaI_2 and $Ca(CF_3SO_3)_2$ are not significantly affected, while most of $Ca(TFSI)_2$ undergoes degradation. The POE-CaI_2 polymer electrolytes exhibit the lowest T_{onset} ~ 350°C. This evidence is ascribed to the reaction between the degradation byproducts of POE and CaI_2, which releases I_2. The latter is easily removed, as it already undergoes sublimation at room temperature and is characterized by a boiling point (B_p) equal to 183°C. Since POE-CaI_2 polymer electrolytes do not lose weight below 350°C, I_2 is not produced in the

operating temperature range of solvent-free batteries. Accordingly, CaI_2 is applicable in Ca polymer electrolytes.

With respect to the pristine POE host, the introduction of CaX_2 salts raises the temperature of the weight loss by *ca.* 100°C. This does not mean that thermal degradation is delayed by the presence of the CaX_2 salts, but rather that the volatile degradation byproducts interact with Ca salts, increasing their volatilization temperature [26]. It is worth to highlight that TGA analyses discussed so far were carried out under an inert atmosphere. These conditions reflect neither the real atmosphere in a battery, nor the conditions after its failure. Furthermore, scanning experiments such as those discussed so far do not allow achieving reliable information on how the weight loss at a given temperature depends on time. To address these issues, isothermal studies were carried out in the presence of oxygen. Figure 3 displays the weight losses of POE-$Ca(CF_3SO_2)_2$ at 100°C and 170°C. It is shown that the onset of the thermal degradation occurs at much lower temperatures than those listed in Table 3. A negligible weight loss of less than 0.5% was noticed at 100°C. With this thermal stability, POE-$Ca(CF_3SO_2)_2$ and most likely also the other POE-CaX_2 polymer electrolytes can be used in a battery operating at temperatures at least as high as 100°C. On the other hand, Table 3 reveals that these polymer electrolytes are thermally unstable at 170°C since they exhibit an average weight loss of 2.8% per hour. Indeed, in the case of an exothermal event, the temperature of the battery can reach and even exceed 170°C. It is emphasized that in the first hour at T = 170°C only 0.9% of volatile, thus easily flammable byproducts are released. This is not an absolute safety guarantee, but must be compared to the low Flash Point (F_p) of liquid electrolytes used in conventional lithium batteries. One example is dimethyl carbonate, DMC, whose F_p is approximately ~17ºC.

3.4. Thermomechanical behavior of POE-$Ca(CF_3SO_3)_2$ electrolytes

The mechanical properties of POE-$Ca(CF_3SO_3)_2$ electrolytes were studied by DMTA as a function of the temperature and of the concentration of dissolved $Ca(CF_3SO_3)_2$. Figure 4 shows the storage modulus (E') as a function of the temperature for samples with different O/Ca ratios.

In the vitreous state, E' ranges between 4.4 and 5.1 GPa. In accordance with the concentration of $Ca(CF_3SO_3)_2$, E' decreases as the salt concentration raises, since a decrease in crystallinity is produced, as previously stated through the DSC analysis.

The glass-rubber transition is marked by: (i) a clear drop of the storage modulus; and (ii) a peak in the tan δ signal, whose maximum is associated to the nominal glass transition temperature, T_α, reflecting the segmental mobility of the polymer electrolytes. Since T_g values measured from DSC are artificially increased by the constraining caused by the crystalline regions, they are investigated by DMTA on samples that had not undergone any thermal treatment and, accordingly, were in their pristine state. In general, T_α values are significantly higher than the T_g measured by DSC. A similar evidence, consisting of a gap of *ca.* 15°C between T_α and T_g, was recently observed on poly(oxyethylene) networks having much lower crystallinity and T_m [33] than the POE homopolymer.

For samples reported in Figure 4, T_α values slightly shift to higher temperatures (up to ~ 10°C), whereas the tan δ peak becomes gradually higher and broader as the salt concentration increases. In semi-crystalline polymers the behavior of tan δ illustrates only the segmental dynamics of the amorphous regions. Thus, it is generally observed that the amplitude of tan δ evolves, becoming sharper and more intense, as the crystallinity degree decreases. Thus, the tan δ behavior revealed by the POE-$Ca(CF_3SO_3)_2$ polymer electrolytes may arise from the fact that the decrease of crystallinity, which normally

facilitates the increase of the segmental mobility when the salt is less diluted, may be counterbalanced by stronger interactions between the salt and the polymeric macromolecular solvent. Since the mechanical strength is mainly dependent on the crystalline phase, the storage modulus drops dramatically above the melting temperature, leading to creeping phenomena as $T \geq 80°C$. The evolution of E' was studied up to 100°C to reveal possible transient crosslinking triggered by the divalent nature of the cations and ascribable to Ca^{2+} interchain solvation. For that purpose, POE-$Ca(CF_3SO_3)_2$ and POE-$Mg(CF_3SO_3)_2$ samples with different salt concentrations were compared. Although in the range of uncertainties, two trends can be highlighted. First, for both alkaline-earth based POE electrolytes, creeping decreases as the salt concentration lowers. For all salt concentrations, the resistance to creeping of POE-$Mg(CF_3SO_3)_2$ is higher than that of POE-$Ca(CF_3SO_3)_2$. This is in agreement with the higher hardness (HSAB theory) of Mg *vs* Ca and also with the mechanical strength improvement induced by stronger magnesium-oxygen bonds (Mg-O) [34]. However, despite the divalent nature of Ca^{2+} and Mg^{2+}, this resistance to creeping is not as high as that previously observed for POE-$NaCF_3SO_3$ (O/Na = 20). Indeed, in that case, E' reached values up to 98 MPa at 80 °C [26]. Even though the mechanical analyses only provide macroscopic descriptions of a given material, one can assume that if both Ca^{2+} and Mg^{2+} benefit from interchain and intrachain solvation, the latter is not predominant. Moreover, early studies [35][36] dealt with a POE complex including $HgCl_2$. In such systems, Hg^{2+} was located in a POE helix, highlighting that solvation by POE of divalent cations may lead to a complex amorphous phase dynamic.

3.5. Ionic conductivity

The conductivity studies were carried out by Electrochemical Impedance Spectroscopy (EIS) in the frequency and temperature range of 1 Hz – 10 MHz and 20 – 90°C, respectively. The profile of the real component of the complex conductivity (σ') as a function of frequency and temperature, for three selected compositions based on $Ca(CF_3SO_3)_2$ is shown in Figure 5.

The profile of the real component of conductivity presents a plateau, corresponding to the global ionic conductivity, which shifts to higher values as temperature increases and to higher frequency as the O/Ca ratio increases.

The trend of global ionic conductivity as a function of temperature and salt concentration during heating for samples based on $Ca(CF_3SO_3)_2$ is reported in Figure 6.

At 20°C, all POE- $Ca(CF_3SO_3)_2$ samples exhibit a very low conductivity, in agreement with the semi-crystalline nature of the polymer electrolyte. The ionic conductivity increases as the temperature raises for all O/Ca ratios. Conductivity maxima were reached at 90ºC and ranged from 0.23 $mS \cdot cm^{-1}$ (O/Ca=8) to 0.47 $mS \cdot cm^{-1}$ (O/Ca=30 very close to O/Ca =40). In this sense, it must be emphasized that, with respect to POE-$LiCF_3SO_3$ electrolytes, the ionic conductivity of POE-$Ca(CF_3SO_3)_2$ electrolytes is significantly higher [37]. In both liquid and polymer electrolytes, the conductivity depends on both the salt concentration and the mobility of the ions. As the concentration of salt in the electrolyte raises, the concentration of mobile ions is globally increased; at the same time, the ion pair dissociation and the mobility of the ions is decreased; consequently, the viscosity of liquid electrolytes raises and the segmental motion in solvent-free polymer electrolytes is inhibited. As a result of these opposite phenomena, in both liquid and polymer electrolytes, the ionic conductivity reaches a maximum at a specific concentration of salt. The highly concentrated sample characterized by an O/Ca ratio of 8 creeps at high temperature. On the other hand, from the conductivity plots it can be

assumed that the other compositions do not creep in the explored temperature range. Therefore, the highest conductivity (that reached 0.47 $mS \cdot cm^{-1}$), was obtained for the concentrations of $Ca(CF_3SO_3)_2$ corresponding to O/Ca = 30, even though the gap with the lowest one i.e. O/Ca = 8 barely exceeds a factor 2. Nonetheless, as the Ca^{2+} charge is twice that of Li^+, these concentrations are comparable to those corresponding to a O/Li = 15 or 4, while the practical salt concentrations in Li-polymer batteries range between 20 and 30. As compared to the conductivities reported for the CAPEs based on poly(PEG-di-acrylate) network and calcium nitrate [24], our CAPE of concentration O/Ca =30 leads, at 90°C, to conductivity values roughly ten times higher than those obtained for Li-PE with an equivalent O/Li ratio. This can be ascribed both to the higher dissociation of Ca triflate compared to Ca nitrate and to the high crosslink density of network. Regarding CAPE based on poly(oxytetramethylene) i.e. PTHF co-crosslinked with di-epoxy [23], the less concentrated CAPE i.e. O/Ca=13.8 barely approaches 0.1 mS/cm at 90ºC. Due to a lesser solvating repeat unit than POE (lower DN), PTHF networks were found to provide with LiTFSI, conductivities one order of magnitude lower [38]. In ref. [23], the oligoTHF curing provides however, in average, through the di-epoxy ring opening 4 OH group per kg increasing the AN of the network, thus its solvating ability. Comparing our data with the few ones available reinforce our selection of a host polymer based on oxyethylene repeat unit.

Data presented in Figure 6 were fitted by using the Vogel-Tamman-Fuelcher (VTF) equation as elsewhere described [39]:

$$\sigma(T) = A_0 T^{-1/2} \left(\frac{-E_a}{R(T-T_0)}\right) \qquad \text{(eq. 2)}$$

where $A_{0,i}$ is proportional to the number of charge carriers, $E_{a,i}$ is the pseudo-activation energy for conduction and $T_{0,i}$ is the ideal thermodynamic glass transition temperature. The pseudo-activation energy of conductivity is similar for all the Ca/O ratios (ca. 14.3 kJ/mol) with the exception of Ca/O = 16 (19.2 kJ/mol). These values are in accordance with other studies for systems based on POE and $LiClO_4$ [40].

We extended this study to both POE-CaI_2 and POE-$Ca(TFSI)_2$ electrolytes, where O/Ca = 30 and 40, corresponding to a Li polymer electrolyte of 15 and 20 respectively. In addition to its intrinsic stability in reduction, CaI_2 has two main advantages, namely its molar weight 294 g as compared to 338 g for $Ca(CF_3SO_3)_2$ and 600 g for $Ca(TFSI)_2$ and its low cost. Regarding $Ca(TFSI)_2$, it was chosen to achieve a good comparison with LiTFSI considered, since early work [41], as the reference salt in Li-POE electrolytes. Figure 7 compares the Arrhenius plots of POE electrolytes based on CaI_2 and $Ca(TFSI)_2$. Unfortunately, POE-CaI_2 exhibits poor conductivities, slightly exceeding 0.01 mS at 85ºC for the ratio O/Ca = 40. On the other hand, POE-$Ca(TFSI)_2$ polymer electrolytes revealed ionic conductivities higher than those obtained with POE-$Ca(CF_3SO_3)_2$. Indeed, at 90°C, the maxima ranged from 0.82 $mS \cdot cm^{-1}$ (O/Ca = 30) to 0.48 $mS \cdot cm^{-1}$ (O/Ca = 40). However, these values are questionable as creeping occurs from 80 to 85ºC for O/Ca 30 and 40, respectively. From these preliminary data, it can be inferred that $Ca(CF_3SO_3)_2$ is the most suitable among the investigated Ca salts, in terms of conductivity, molar weight and electrochemical window. Moreover, based on data obtained in Li-polymer electrolytes, where the cationic transference number (T^+) of $LiCF_3SO_3$ is roughly 3 times higher than that of LiTFSI [42], higher T^+ and, consequently, higher cationic conductivity, σ^+, can be expected for POE-$Ca(CF_3SO_3)_2$ electrolytes.

3.6. Discussion

Decreasing the flammability of high-capacity batteries is an important and current challenge for their application in the automotive field and grid implementations. Whereas in Li and Na batteries solid inorganic electrolytes can be a solution to improve safety, as of today no ceramic or glassy electrolyte allows multivalent cations to move at least, in the explored temperature range. This preliminary study validates the possibility to dissolve, up to fairly high salt concentrations, three calcium salts in the reference host polymer, POE. The choice of POE is dictated by the state of the art in lithium polymer electrolytes. Indeed, it is assumed that if POE has demonstrated sufficient electrochemical stability *vs* Li metal, it could be advantageously used with Ca metal. Additionally, POE homo- and copolymers have an anodic stability close to 3.9 V *vs* Li/Li^+ thus 3.72 V *vs* Ca/Ca^{2+}. Hence, they could be electrochemically stable with several cathodes previously proposed. Thus, Ca^{2+} was reversibly inserted in nanocrystallized V_2O_5 [43] while enhanced insertion in V_2O_5 nanocomposites compared to Li [44] was reported, validating the capability of CaB to benefit from high-performing positive electrode materials. Even though these validations were performed using liquid electrolytes, Gauthier *et al.* [45] built and successfully tested Li/VO_x prototypes based on solvent-free polymer salt complexes used both as polymer electrolytes and as binders of $LiVO_x$ composite cathodes, paving the way for the use of CAPE as binders for V_2O_5 cathode materials. Whether the present work illustrates the feasibility in terms of salt solubility and conductivity of POE electrolytes, it however also emphasizes their limitations in terms of (i) crystallinity and T_m and (ii) mechanical properties (creeping from 80 to 85°C). These limitations could be overcome by using amorphous polyether networks, which demonstrated high conductivities as Li polymer electrolytes, while avoiding creeping [33]. Nonetheless, information about cationic transference numbers, T^+ is missing in this paper as their determination currently faces two issues: (i) Ca^{2+} does not deposit onto Ca^0;

this hinders the electrochemical determination from symmetric Ca^0/Ca-electrolyte/ Ca^0 cells [46[47]; and (ii) the inadequacy of Pulse Field Gradient NMR as a characterization technique, as the main Ca isotope is not detected by NMR. Nonetheless, a cationic transference number has recently been measured [23] using the impedance technique [47]. This measurement at least exists even though we are fully convinced neither by the shape of the polarization curve [23] (see supplementary information) nor by the establishment of a steady-state current. Moreover the fairly high T^+ reported, 0.352, was obtained for the concentration O/Ca = 1.9 (similar to O/Li #1) far from the usual salt concentrations in polymer electrolyte-based batteries, falling more within the salt in polymer concept. Regarding the mobility of alkaline-earth cations, Vincent reported that Mg^{2+} moves together with oligoether chains having molecular weights below the entanglement threshold (~3,200 g·mole^{-1}) [48]. He also compared, by *d.c.* polarization [49], the mobility of Mg^{2+} and Ca^{2+} hosted in oligomers (M_n >> 3,200 g) and linear polymers (commercial POE and polycondensates), using mercury amalgams (Mg/Hg and Ca/Hg) electrodes. Surprisingly, Vincent did not use the impedance technique that he previously co-authored [47] to access T^+. In both host polymers, Mg^{2+} was found to be immobile. Conversely, an important current passed for more than 20 hours in the calcium symmetric cell. Indeed, if alkaline cations, from Li^+ to K^+, and alkaline-earth cations, from Mg^{2+} to Ba^{2+} are both considered as Hard Acids (HSAB theory), one can infer that Li^+ should have roughly the same hardness as Mg^{2+} when Ca^{2+} hardness should be close to K^+ one. Since the ether function of ethylene oxide repeat unit is a Hard Base, a high Acid Hardness should be more detrimental to the mobility of alkaline-earth cations compared to alkaline cations, especially as the former have a double positive charge. Besides Vincent, on the basis of water molecules exchanges, assumed a higher hardness of Mg^{2+} *vs* Ca^{2+}, assumption in accordance with the reinforcement of thermoplastics,

elastomers and gels induced by MgO fillers [34]. A significant reinforcement above T_m, with regard to POE host, should be therefore induced by the dissolution of Ca and, above all, of Mg salts. Nonetheless, even though both Ca^{2+} and Mg^{2+} triflate delay the creeping of their related polymer electrolytes with regard to the POE host, this reinforcement, even in the case of Mg triflate, is not noticeable with regard to POE/Na triflate [26] (*vide supra*). As a tentative explanation, one can infer that both divalent cations are mainly located inside POE (intra-chain solvation) minimizing inter-chain solvation and, therefore, transient crosslinks. Based on macroscopic, *therefore questionable*, DMTA data, this assumption is however supported by the crystallographic structure of POE/$HgCl_2$ complexes [35][36].

4. Conclusions

The experimental data presented in this work validate the use of liquid-free CAPE based on the reference and commercially available poly(oxyethylene) (POE). All the calcium salts tested in this work were found to be homogeneously dissolved in the POE host polymer and we did not detect any microphase separation. The thermal stability of Ca polymer electrolytes points to a very high level of safety; the conductivity levels beyond the melting temperature, though not outstanding, are satisfactory for the intended application. However, the proposed CAPE suffer from two main drawbacks: (i) low conductivities from ambient temperature to T_m; and (ii) an insufficient mechanical strength, that prevents their processing into thin films. After validating the suitability of POE chains as a macromolecular solvent, from now on we are aiming at improving room temperature conductivities by using amorphous polyether networks prepared either from polycondensates [33] or from POE copolymers [50][51]. Although these networks, due to their three-dimensional nature, would allow the polymer electrolyte creeping to be

avoided, their processing into films 10 to 20 µm thick is challenging as it requires a high density of crosslinks, that is detrimental to ionic conductivity [23][24]. Nevertheless, nanocomposite strategies [52] based on the use of moderate wt% amounts of Crystalline Nano Cellulose (CNC) should reconcile a high mechanical strength and high conductivities, allowing the ohmic drop in the electrolyte to be decreased. Contrarily to Li and even Na polymer electrolytes, the development of CAPEs still remains a pioneering topic that requires intensive research efforts, *e.g.* exploration of new salts benefiting from extended delocalization of the anionic charge [53], accurate determination of cationic transference numbers, studies to elucidate the evolution of the interface between Ca^0 and CAPEs based on various Ca salts, etc. This physicochemical work paves the way for the development of improved polymer electrolytes able to conduct Ca species.

Acknowledgements

This project has received funding from the European Union's Horizon 2020 research and innovation programme under grant agreement No 829145 (FETOPEN-VIDICAT).

V. Di Noto thanks the University Carlos III of Madrid for the "Cátedras de Excelencia UC3M-Santander" (Chair of Excellence UC3M-Santander).

References

[1] C. Pillot, Lithium ion battery raw material supply & demand 2016-2025, Avicenne Energy, 2017, www.avicenne.com.

[2] J.M. Gitlin, Germany's Bundesrat votes to ban the internal combustion engine by 2030, Ars Tech. (2016). https://arstechnica.com/cars/2016/10/germanys-bundesrat-votes-to-ban-the-internal-combustion-engine-by-2030/ (accessed July 26, 2019).

[3] A. Chrisafis, A. Vaughan, France to ban sales of petrol and diesel cars by 2040, Guard. (2017). https://www.theguardian.com/business/2017/jul/06/france-ban-petrol-diesel-cars-2040-emmanuel-macron-volvo (accessed July 26, 2019).

[4] G. De Clercq, French renewables power grid pilot shows limits of batteries in Europe, Reuters. (2015). http://www.reuters.com/article/us-utilities-grids-france/french-renewables-power-grid-pilot-shows-limits-of-batteries-in-europe-idUSKCN0PF06M20150705 (accessed July 26, 2019).

[5] A. Opitz, P. Badami, L. Shen, K. Vignarooban, A.M. Kannan, Can Li-Ion batteries be the panacea for automotive applications?, Renew. Sustain. Energy Rev. 68 (2017) 685–692. doi:10.1016/j.rser.2016.10.019

[6] Y. Barsukov, J. Qian, Battery Power Management for Portable Devices, Artech Hou, Artech House Power Engineering, Norwood M. A., 2013

[7] F. Lambert, Electric vehicle battery cost dropped 80% in 6 years down to $227/kWh – Tesla claims to be below $190/kWh, Electrek. (2017). https://electrek.co/2017/01/30/electric-vehicle-battery-cost-dropped-80-6-years-227kwh-tesla-190kwh/ (accessed July 26, 2019).

[8] B. Nykvist, M. Nilsson, Rapidly falling costs of battery packs for electric vehicles, Nat. Clim. Chang. 5 (2015) 329–332. doi:10.1038/nclimate2564.

[9] D.L. Wood, J. Li, C. Daniel, Prospects for reducing the processing cost of lithium ion batteries, J. Power Sources. 275 (2015) 234–242. doi:10.1016/j.jpowsour.2014.11.019.

[10] J. Park, Z. Xu, G. Yoon, S.K.Park, J. Wang, H. Hyun, H. Park, J. Lim, Y-J. Ko, Y.S. Yun, K. Kang, Stable and high-power calcium-ion batteries enabled by calcium intercalation into Graphite, Adv. Mat. 32 (2020) 1904411. Doi: 10.1002/adma.201904411.

[11] E. Peled, The Electrochemical Behavior of Alkali and Alkaline Earth Metals in Nonaqueous Battery Systems—The Solid Electrolyte Interphase Model, J. Electrochem. Soc. 126 (1979) 2047. doi:10.1149/1.2128859.

[12] E. Peled, E. Elster, R. Tulman, J. Kimel, Calcium/Ca(AlCl4)2 - Thionyl Chloride high-rate (TC)cell. Effect of temperature and cell parameters on performance, J. Power Sources. 14 (1985) 93–98. doi:10.1016/0378-7753(85)88017-4.

[13] E. Peled, A. Meitav, M. Brand, Calcium Thionyl Chloride High-Rate Reserve Cell, J. Electrochem. Soc. 128 (1981) 1936. doi:10.1149/1.2127768.

[14] K.A. See, J.A. Gerbec, Y.S. Jun, F. Wudl, G.D. Stucky, R. Seshadri, A high capacity calcium primary cell based on the Ca-S system, Adv. Energy Mater. 3 (2013) 1056–1061. doi:10.1002/aenm.201300160.

[15] D. Aurbach, R. Skaletsky, Y. Gofer, The Electrochemical Behavior of Calcium Electrodes in a Few Organic Electrolytes, J. Electrochem. Soc. 138 (1991) 3536. doi:10.1149/1.2085455.

[16] H. Kim, D.A. Boysen, D.J. Bradwell, B. Chung, K. Jiang, A.A. Tomaszowska, K. Wang, W. Wei, D.R. Sadoway, Thermodynamic properties of calcium-Bismuth alloys determined by emf measurements, Electrochim. Acta. 60 (2012) 154–162. doi:10.1016/j.electacta.2011.11.023.

[17] H. Kim, D.A. Boysen, T. Ouchi, D.R. Sadoway, Calcium-bismuth electrodes for large-scale energy storage (liquid metal batteries), J. Power Sources. 241 (2013) 239–248. doi:10.1016/j.jpowsour.2013.04.052.

[18] A. Ponrouch, C. Frontera, F. Bardé, M.R. Palacín, Towards a calcium-based rechargeable battery, Nat. Mater. 15 (2016) 169–172. doi:10.1038/nmat4462

[19] D. Wang, X. Gao, Y. Chen, L. Jin, C. Kuss, P.G. Bruce, Plating and stripping calcium in an organic electrolyte, Nat. Mater. 17 (2018) 16–20. doi:10.1038/NMAT5036.

[20] A. Ponrouch, R.Palacin, Current Opinion in Electrochemistry, 10.1016/j.coelec.2018.02.001

[21] J. Muldoon, C.B. Bucur, T. Gregory, Quest for nonaqueous multivalent secondary batteries: Magnesium and beyond, Chem. Rev. 114 (2014) 11683–11720. doi:10.1021/cr500049y..

[22] C. Martinez-Cisneros, C. Antonelli, A. Fernandez-Gorgojo, B. Levenfeld, A. Varez, J.-Y. Sanchez, From lithium to post-lithium batteries: Na & Ca conducting solvent-free polymer electrolytes, (2016). Conference at XXXVII Reunión del Grupo de Electroquímica de la Real Sociedad Española de Química, Alicante, Spain.

[23] J. Wang, F.S. Genier, H. Li, S. Biria, I.D. Hosein, A Solid Polymer Electrolyte from Cross-Linked Polytetrahydrofuran for Calcium Ion Conduction, ACS Appl. Polym. Mater. 1 (2019) 1837–1844. doi:10.1021/acsapm.9b00371

[24] F.S. Genier, C. V. Burdin, S. Biria, I.D. Hosein, A novel calcium-ion solid polymer electrolyte based on crosslinked poly(ethylene glycol) diacrylate, J. Power Sources. 414 (2019) 302–307. doi:10.1016/j.jpowsour.2019.01.017.

[25] C. Vachon, C. Labrèche, A. Vallée, S. Besner, M. Dumont, J. Prud'homme, Microphase Separation and Conductivity Behavior of Poly(propylene oxide)-Lithium Salt Electrolytes, Macromolecules. 28 (1995) 5585–5594. doi:10.1021/ma00120a025

[26] C.S. Martinez-Cisneros, B. Levenfeld, A. Varez, J.Y. Sanchez, Development of sodium-conducting polymer electrolytes: Comparison between film-casting and films obtained via green processes, Electrochim. Acta. 192 (2016) 456–466. doi:10.1016/j.electacta.2016.02.011.

[27] B. Bhattacharya, R.K. Nagarale, P.K. Singh, Effect of sodium-mixed anion doping in PEO-based polymer electrolytes, High Perform. Polym. 22 (2010) 498–512. doi:10.1177/0954008309104931.

[28] S.A.M. Noor, A. Ahmad, M.Y.A. Rahman, I.A. Talib, Solid polymeric electrolyte of poly (ethylene) oxide-50 % epoxidized natural rubber-lithium triflate, Nat. Sci. 2 (2010) 190–196. doi:10.4236/ns.2010.23029.

[29] F. Bossard, N. El Kissi, A. D'Aprea, F. Alloin, J.Y. Sanchez, A. Dufresne, Influence of dispersion procedure on rheological properties of aqueous solutions of high molecular weight PEO, Rheol. Acta. 49 (2010) 529–540. doi:10.1007/s00397-009-0402-8.

[30] J. Lipkowski, P.N. Ross, Frontiers in Electrochemistry, Volume 3: The electrochemistry of novel materials, New York, 1994.

[31] M.A. Mehta, P. Lightfoot, P.G. Bruce, Phase Diagram of the Poly(ethylene oxide):Ca(CF3SO3)2 System, Chem. Mater. 5 (1993) 1338–1343. doi:10.1021/cm00033a026..

[32] A. Vallée, S. Besner, J. Prud'Homme, Comparative study of poly(ethylene oxide) electrolytes made with LiN(CF3SO2)2, LiCF3SO3 and LiClO4: Thermal properties and conductivity behaviour, Electrochim. Acta. 37 (1992) 1579–1583. doi:10.1016/0013-4686(92)80115-3.

[33] A. Thiam, C. Antonelli, C. Iojoiu, F. Alloin, J.Y. Sanchez, Optimizing ionic conduction of poly(oxyethylene) electrolytes through controlling the cross-link density, Electrochim. Acta. 240 (2017) 307–315. doi:10.1016/j.electacta.2017.04.046.

[34] N. Wu, W. Wang, Y. Wei, T. Li, Studies on the effect of nano-sized MgO in magnesium-ion conducting gel polymer electrolyte for rechargeable magnesium batteries, Energies. 10 (2017). doi:10.3390/en10081215.

[35] A.A. Blumberg, S.S. Pollack, C.A.J. Hoeve, A poly(ethylene oxide)–mercuric chloride complex, J. Polym. Sci. Part A Gen. Pap. 2 (1964) 2499–2502. doi:10.1002/pol.1964.100020601.

[36] M. Yokoyama, H. Ishihara, R. Iwamoto, H. Tadokoro, Structure of Poly (ethylene oxide) Complexes. III. Poly (ethylene oxide)-Mercuric Chloride Complex. Type II, Macromolecules. 2 (1969) 184–192. doi:10.1021/ma60008a016.

[37] T. Caruso, S. Capoleoni, E. Cazzanelli, R.G. Agostino, P. Villano, S. Passerini, Characterization of PEO-Lithium Triflate Polymer Electrolytes: Conductivity, DSC and Raman Investigations, Ionics (Kiel). 8 (2002) 36–43. doi.org/10.1007/BF02377751.

[38] F. Alloin, J.-Y. Sanchez, Electrochemical comparison of several cross-linked polyethers, Electrochim. Acta. 43 (1998) 1199–1204. doi:10.1016/S0013-4686(97)10020-2.

[39] V. Di Noto, G.A. Giffin, K. Vezzù, M. Lavina, S. Piga, Broadband Dielectric Spectroscopy: A Powerful Tool for the Determination of Charge Transfer Mechanisms in Ion Conductors, in: P. Knauth, M.L. Di Vona (Eds.), Solid State Prot. Conduct. Prop. Appl. Fuel Cells, John Wiley & Sons, Ltd, 2012: p. 426. doi:10.1002/9781119962502.ch5.

[40] K. Vezzù, V. Zago, M. Vittadello, A. Bertucco, V. Di Noto, Effect of subcritical CO2 on ionic conductivity of {Al[O(CH2CH2O)8.7]ρ (LiClO4)z}n hybrid inorganic–organic networks, Electrochim. Acta. 51 (2006) 1592–1601. doi:10.1016/j.electacta.2005.06.039.

[41] S. Sylla, J.Y. Sanchez, M. Armand, Electrochemical study of linear and crosslinked POE-based polymer electrolytes, Electrochim. Acta. 37 (1992) 1699–1701. doi:10.1016/0013-4686(92)80141-8.

[42] F. Alloin, D. Benrabah, J.-Y. Sanchez, Comparative ion transport in several polymer electrolytes, J. Power Sources. 68 (1997) 372–376. doi:10.1016/S0378-7753(97)02536-6.

[43] G.G. Amatucci, F. Badway, A. Singhal, B. Beaudoin, G. Skandan, T. Bowmer, I. Plitz, N. Pereira, T. Chapman, R. Jaworski, Investigation of Yttrium and Polyvalent Ion Intercalation into Nanocrystalline Vanadium Oxide, J. Electrochem. Soc. 148 (2001) A940. doi:10.1149/1.1383777.

[44] M. Bervas, L.C. Klein, G.G. Amatucci, Vanadium oxide-propylene carbonate composite as a host for the intercalation of polyvalent cations, Solid State Ionics. 176 (2005) 2735–2747. doi:10.1016/j.ssi.2005.09.009.

[45] M. Gauthier, A. Bélanger, P. Bouchard, B. Kapfer, S. Ricard, G. Vassort, M. Armand, J.Y. Sanchez, L. Krause, Large lithium polymer battery development The immobile solvent concept, J. Power Sources. 54 (1995) 163–169. doi:10.1016/0378-7753(94)02060-G.

[46] P.R. Sørensen, T. Jacobsen, Conductivity, charge transfer and transport number-an ac-investigation of the polymer electrolyte LiSCN-poly(ethyleneoxide), Electrochim. Acta. 27 (1982) 1671–1675. doi:10.1016/0013-4686(82)80162-X.

[47] J. Evans, C.A. Vincent, P.G. Bruce, Electrochemical measurement of transference numbers in polymer electrolytes, Polymer (Guildf). 28 (1987) 2324–2328. doi:10.1016/0032-3861(87)90394-6.

[48] J. Shi, C.A. Vincent, The effect of molecular weight on cation mobility in polymer electrolytes, Solid State Ionics. 60 (1993) 11–17. doi:10.1016/0167-2738(93)90268-8.

[49] C.A. Vincent, Ion transport in polymer electrolytes, Electrochim. Acta. 40 (1995) 2035–2040. doi:10.1016/0013-4686(95)00138-5.

[50] F. Alloin, J.Y. Sanchez, New solvating polyether networks, Electrochim. Acta. 40 (1995) 2269–2276. doi:10.1016/0013-4686(95)00175-E.

[51] F. Alloin, J.-Y. Sanchez, Partial hydrogenation of unsaturated polyethers: a convenient route to curable terpolymers for lithium batteries, J. Polym. Sci. Part A Polym.

Chem. 38 (2000) 2900–2909. doi:10.1002/1099-0518(20000815)38:16<2900::AID-POLA70>3.0.CO;2-2.

[52] M.A.S. Azizi Samir, F. Alloin, J.-Y. Sanchez, A. Dufresne, Cross-Linked Nanocomposite Polymer Electrolytes Reinforced with Cellulose Whiskers, Macromolecules. 37 (2004) 4839–4844. doi:10.1021/ma049504y.

[53] A. Thiam, C. Iojoiu, J.C. Leprêtre, J.Y. Sanchez, Lithium salts based on a series of new anilinyl-perfluorosulfonamide salts and their polymer electrolytes, J. Power Sources. 364 (2017) 138–147. doi:10.1016/j.jpowsour.2017.07.104.

TABLES

Table 1. Relevant properties of Li, Na, K, Mg and Ca for battery applications [10].

Properties	Abundance in Earth's crust (g/kg)	Melting point, T_m (ºC)	Density	Molar mass (g/mol)	Mass-to-electron ratio (g/mol of e^-)	Specific capacity (Ah/g)	Volumetric capacity (Ah/cm^3)	Redox potential (Eo in V *vs* SHE)
Li	0.02	180.5	0.53	6.9	7	3.86	2.06	-3.05
Na	23.6	98.0	0.97	23.0	23	1.16	1.12	-2.71
K	20.9	63.5	0.89	39.1	39	0.68	0.61	- 2.92
Mg	23.3	650	1.74	24	12	2.20	3.80	-2.37
Ca	41.5	842	1.54	40	20	1.34	2.06	-2.87

Table 2. Melting temperature (T_m), melting enthalpy (ΔH_m) and crystallinity (X_c) for POE-based polymer electrolytes at different O/Ca ratios.

O/Ca	**POE-Ca(CF_3SO_3)$_2$**			**POE-CaI_2**			**POE-Ca[TFSI]$_2$**		
	T_m °C	X_c %	ΔH_m J·g^{-1}	T_m °C	X_c %	ΔH_m J·g^{-1}	T_m °C	X_c %	ΔH_m J·g^{-1}
16	52.5	12	26.5	-	-	-	-	-	-
20	54.4	14	30.6	-	-	-	-	-	-
30	59.1	30	64.7	71.5	29	63.9	64.6	18	39.2
40	63.3	34	72.1	69.5	44	95.3	70.8	24	51.1

Table 3. TGA measurements carried out under nitrogen for POE-CaX_2 polymer electrolytes.

POE-CaX_2	T_{onset} (°C)	residue % 450°C	wt% of salt
POE-Ca(CF_3SO_3)$_2$			
O/Ca=8	397.8	51.4	49
O/Ca=16	395.2	36.1	32.4
O/Ca=20	387.5	31.9	27.8
O/Ca=30	386.4	25.1	20.4
O/Ca=40	383.1	21.4	16.1
POE-CaI_2			
O/Ca=30	347.3	21.9	18.2
O/Ca=40	344.6	20.7	14.3
POE-Ca(TFSI)$_2$			
O/Ca=30	357.0	8.3	31.3
O/Ca=40	385.9	8.8	25.4

FIGURES

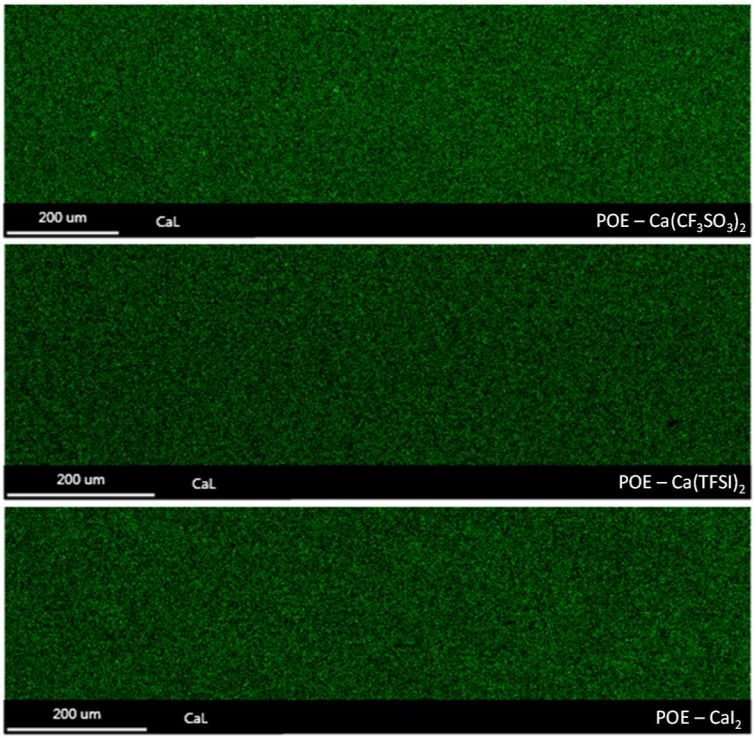

Figure 1. Distribution of calcium obtained by X-ray mapping in the proposed electrolytes. Top panel: POE-$Ca(CF_3SO_3)_2$; middle panel; POE-$Ca(TFSI)_2$; bottom panel: POE-CaI_2. All the samples exhibit an O/Ca molar ratio equal to 30.

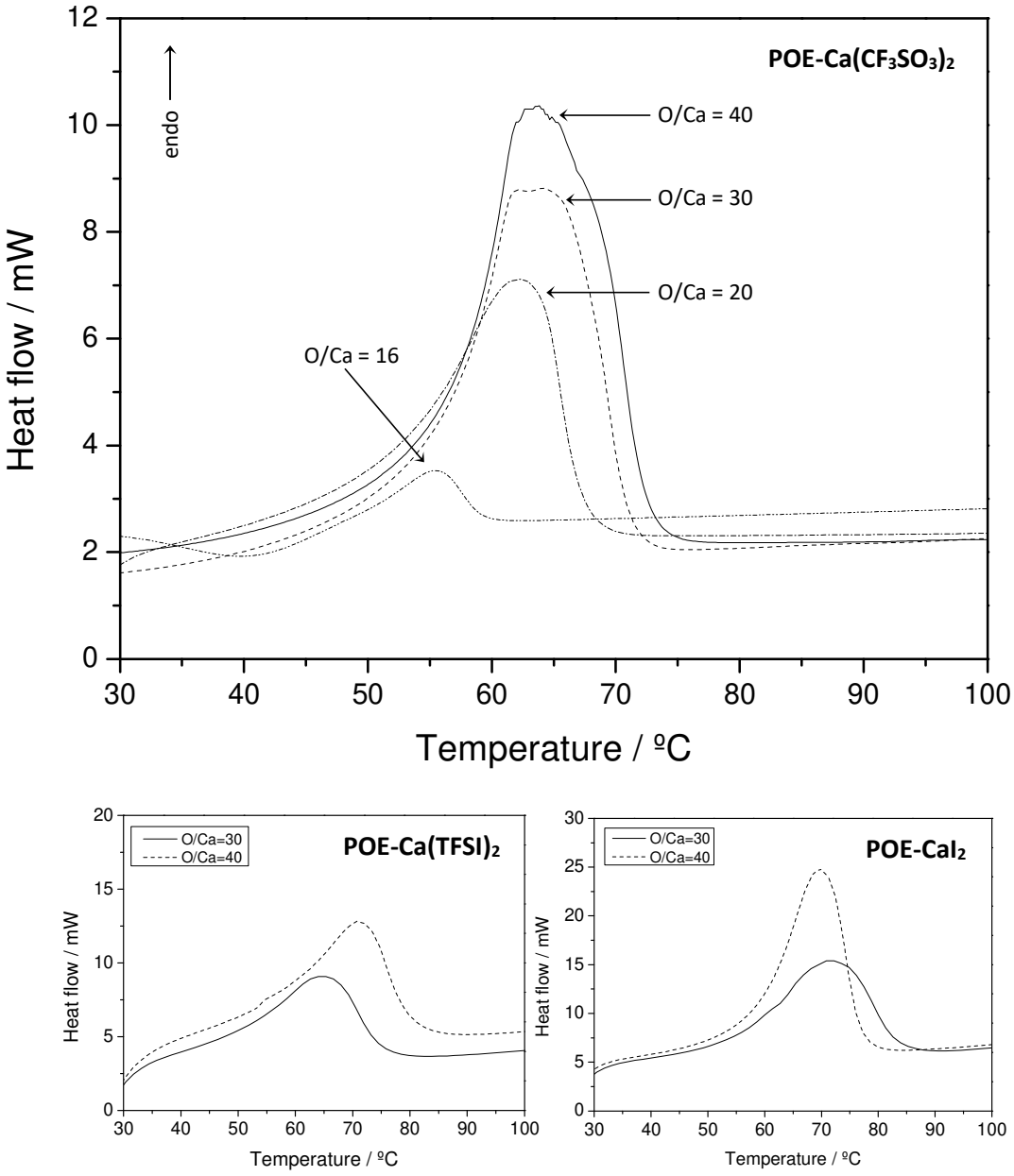

Figure 2. DSC measurements showing the effect of salt concentration and type on melting temperature (T_m) of the different POE-based calcium polymer electrolytes.

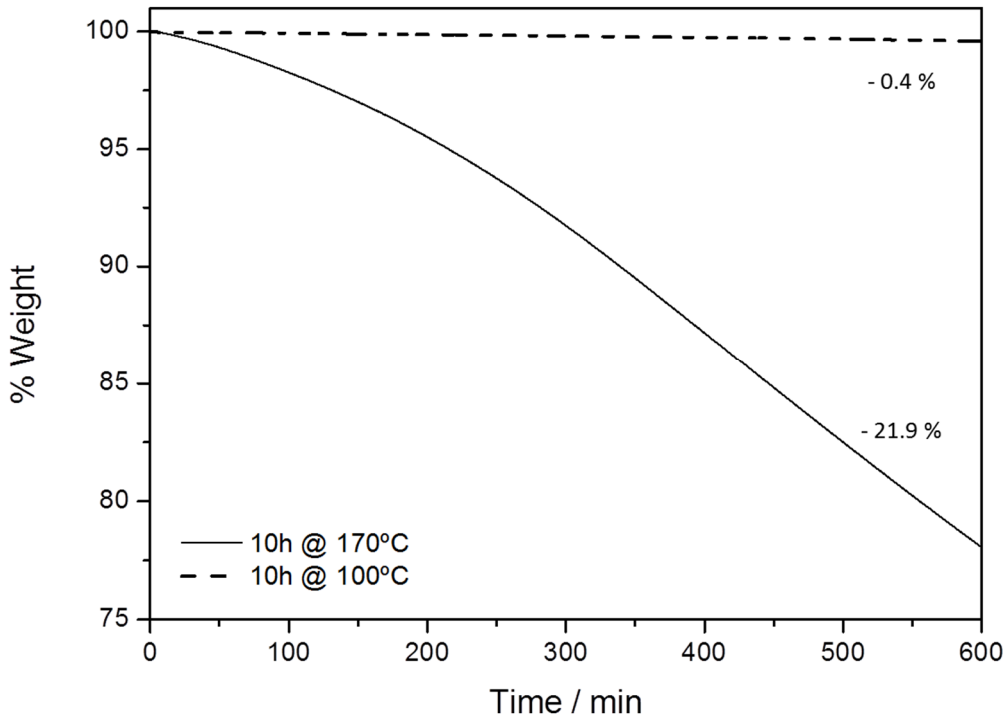

Figure 3. Isothermal TGA analyses of POE-Ca(CF_3SO_3)$_2$ carried out at 100 and 170°C in a mixture of air and nitrogen.

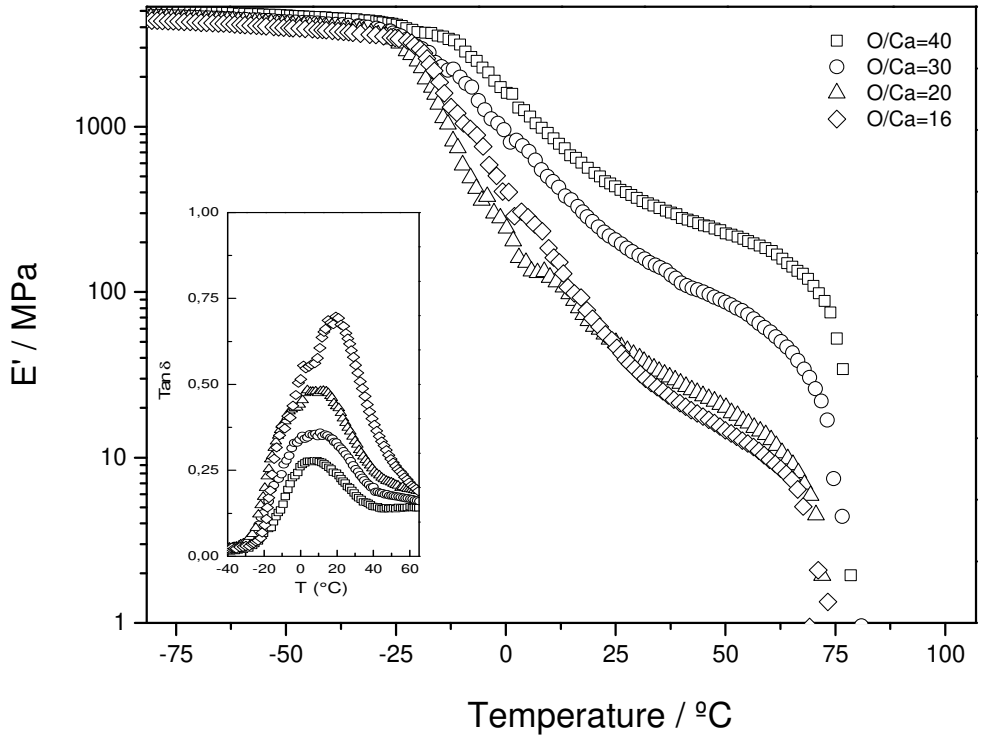

Figure 4. Storage moduli (E') obtained by DMTA for POE-Ca$(CF_3SO_3)_2$ electrolytes at different O/Ca ratios. The inset shows peaks corresponding to the tan δ of the electrolytes as temperature is raised.

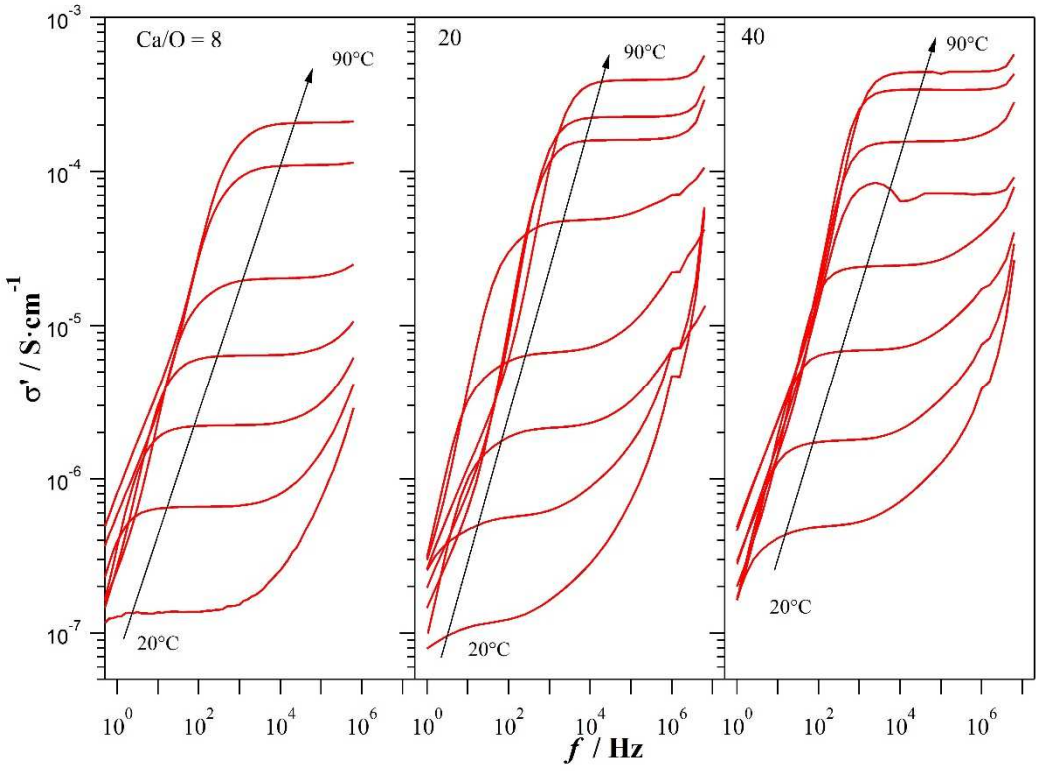

Figure 5. Real component of the complex conductivity (σ') *vs* frequency and temperature for POE-Ca(CF_3SO_3)$_2$ samples (O/Ca = 8, 20, 40).

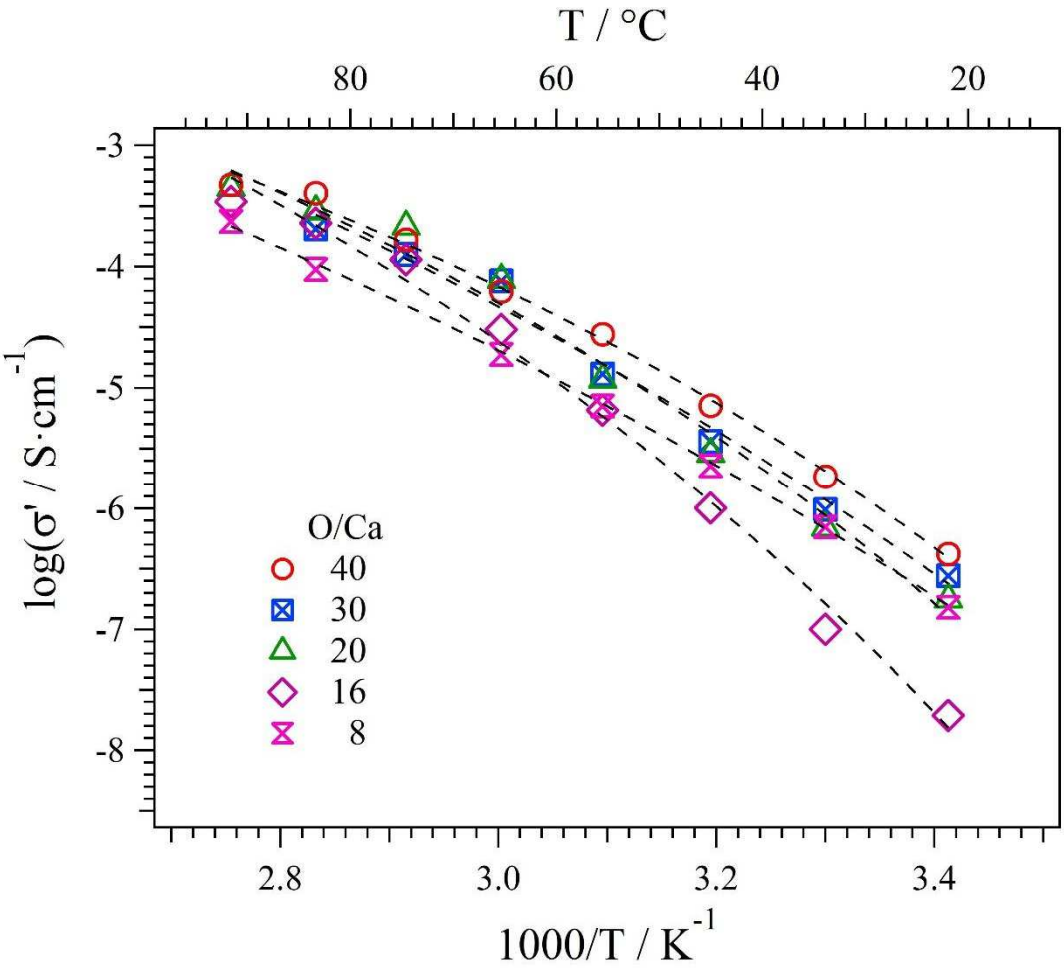

Figure 6. Ionic conductivity as a function of temperature and O/Ca ratio for POE-$Ca(CF_3SO_3)_2$ samples.

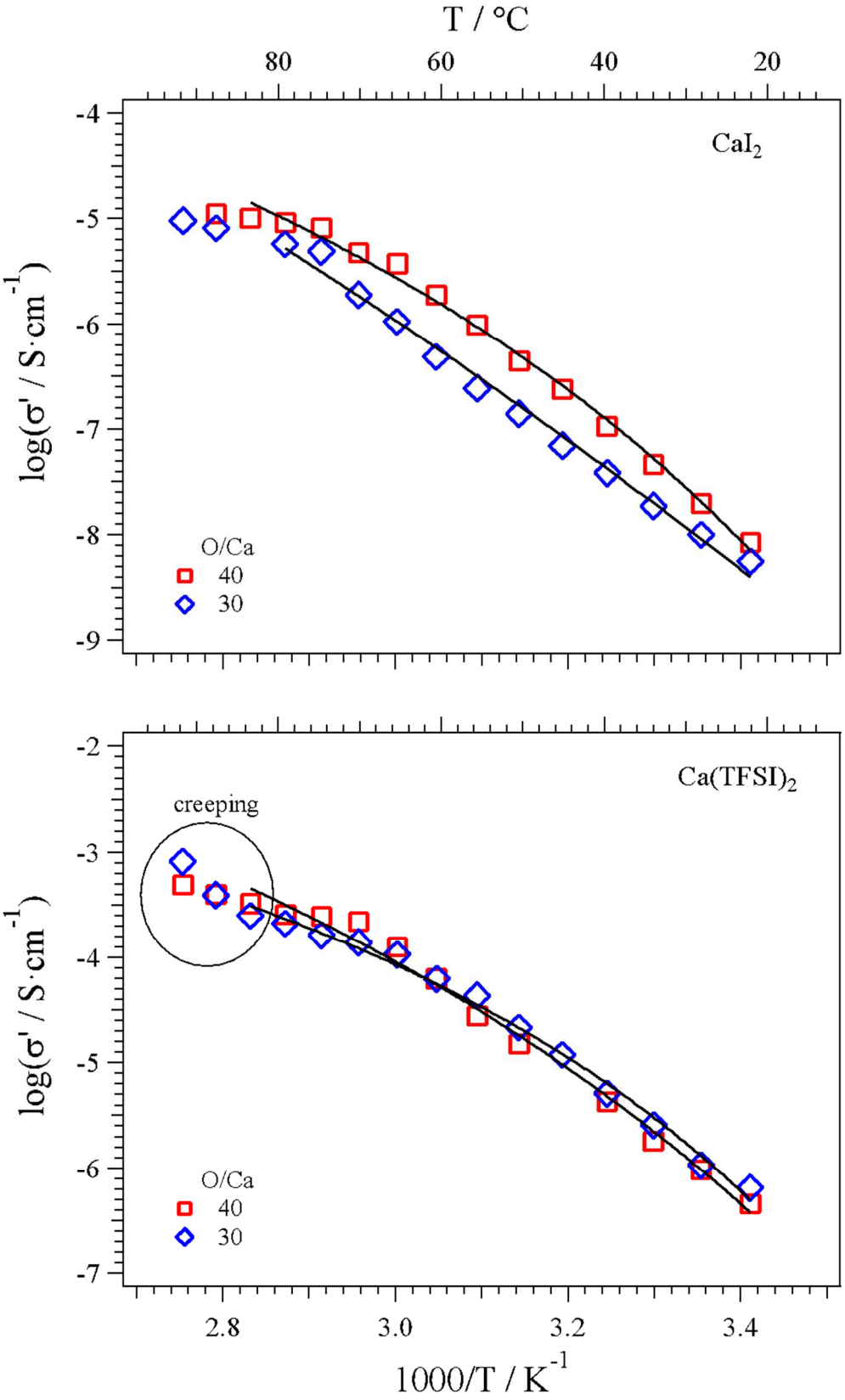

Figure 7. Ionic conductivity as a function of temperature and O/Ca ratio for POE-CaI_2 and POE-$Ca(TFSI)_2$ electrolytes. Dotted lines correspond to VTF fitting.